

See discussions, stats, and author profiles for this publication at: <https://www.researchgate.net/publication/51466442>

Transport of Charged Aerosol OT Inverse Micelles in Nonpolar Liquids

ARTICLE in LANGMUIR · JULY 2011

Impact Factor: 4.46 · DOI: 10.1021/la200424v · Source: PubMed

CITATIONS

18

READS

68

7 AUTHORS, INCLUDING:



Masoumeh Karvar

Ghent University

14 PUBLICATIONS 92 CITATIONS

SEE PROFILE



Filip Strubbe

Ghent University

32 PUBLICATIONS 261 CITATIONS

SEE PROFILE



Filip Beunis

Ghent University

60 PUBLICATIONS 427 CITATIONS

SEE PROFILE



Kristiaan Neyts

Ghent University

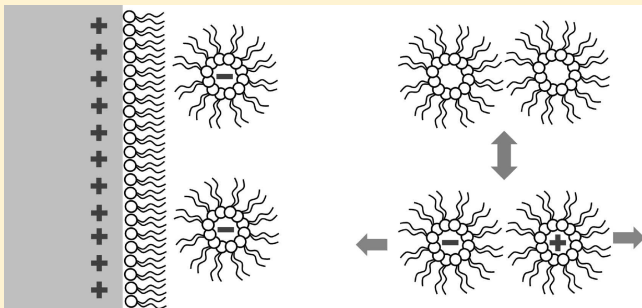
249 PUBLICATIONS 2,068 CITATIONS

SEE PROFILE

Transport of Charged Aerosol OT Inverse Micelles in Nonpolar Liquids

Masoumeh Karvar,^{*,†} Filip Strubbe,[†] Filip Beunis,[†] Roger Kemp,[‡] Ashley Smith,[‡] Mark Goulding,[‡] and Kristiaan Neyts[†][†]Department of Electronics and Information Systems, Ghent University, B-9000 Ghent, Belgium[‡]Merck Chemicals Ltd, University Parkway, Chilworth, Southampton, SO16 7QD, United Kingdom

ABSTRACT: Surfactants such as Aerosol OT (AOT) are commonly used to stabilize and electrically charge nonpolar colloids in devices such as electronic ink displays. The electrical behavior of such devices is strongly influenced by the presence of charged inverse micelles, formed by excess surfactant that does not cover the particles. The presence of charged inverse micelles results in increased conductivity of the solution, affecting both the energy consumption of the device and its switching characteristics. In this work, we use transient current measurements to investigate the electrical properties of suspensions of the surfactant Aerosol OT in dodecane. No particles are added, to isolate the effect of excess surfactant. The measured currents upon application of a voltage step are found to be exponentially decaying, and can be described by an analytical model based on an equivalent electric circuit. This behavior is physically interpreted, first by the high generation rate of charged inverse micelles giving the suspension resistor like properties, and second by the buildup of layers of charged inverse micelles at both electrodes, acting as capacitors. The model explains the measurements over a large range of surfactant concentrations, applied voltages, and device thicknesses.



1. INTRODUCTION

Surfactants in nonpolar liquids are widely used as stabilizers and charging agents for colloidal particles in applications such as motor oil,¹ inkjet printing,² liquid electrostatic developers,³ and electrophoretic ink.^{4–11} Aerosol OT (AOT, or di-2-ethylhexylsulfosuccinate) is an often-used surfactant which has good stabilizing and charging properties and is soluble in many solvents over a wide range of concentrations.^{2,12,13} AOT surfactant molecules in a nonpolar liquid form inverse micelles of which the equilibrium properties, such as micelle size and fraction of charged micelles, are well-studied.^{13–19} A small fraction of the inverse micelles are charged as the result of a disproportionation/comproportionation mechanism in which two neutral inverse micelles exchange a charge, resulting in one negatively and one positively charged inverse micelle (generation), and vice versa (recombination)^{15–17}



The chemical nature or concentration of the ions involved in the charging process (e.g., ionic impurities, traces of water, or even dissociated surfactant molecules) is irrelevant, since they are so abundant that it is rather the concentration of solvating surfactant and the micelle size which determine the conductivity.^{15,20} Therefore, as a result of the mass action law, the conductivity in equilibrium (i.e., in absence of an electric field) is proportional to the number of inverse micelles or to the surfactant concentration if the micelle aggregation number is

assumed to be constant. The fraction of charged inverse micelles is small, on the order of 10^{-5} ,^{15,16} due to their small size compared to the Bjerrum length,²⁰ which is defined as the distance at which the Coulomb interaction energy of two opposite charges is equal to the thermal energy. For dodecane, the nonpolar solvent used in this work, the Bjerrum length is about 28 nm, much larger than the hydrodynamic radius of the micelles of about 1.6 nm.^{16,18} Even with this small fraction of charged inverse micelles, the conductivity is still surprisingly high for a nonpolar liquid, about 5 nS/m per weight percentage AOT added to dodecane.^{15,16}

Charged inverse micelles increase the conductivity of a nonpolar solution and can induce an important electric field when they are separated.^{21,22} In applications such as electrophoretic ink, which are based on the movement of charged pigments in response to an applied voltage, the charged inverse micelles have an important influence on the overall electrical properties and on the particle motion. In these applications, it is therefore essential to understand the behavior of the charged inverse micelles when a voltage is applied.

Transient current measurements, in which a voltage step is applied over a layer of nonpolar liquid with surfactant between parallel electrodes, are useful to study the equilibrium properties of charged inverse micelles, as well as electrodynamic properties

Received: February 1, 2011

Revised: July 4, 2011

Published: July 05, 2011

that go beyond the equilibrium properties. In previous work, we have used this method to study the concentration, mobility, valency, and size of charged polyisobutylene succinimide (PIBS, commercialized as OLOA 1200 by Chevron) inverse micelles, but also to study the generation mechanism of charged inverse micelles and electrodynamics in microscale devices.^{23–27} A model was developed based on drift, diffusion, and generation in the bulk of the liquid and at the interface with electrodes, which explains a wide range of measurements for mixtures of PIBS and dodecane.

In this paper, we report transient current measurements for mixtures of AOT and dodecane with the same aim of studying properties beyond the equilibrium properties, such as charge generation and electrodynamics in a microscale device. However, the results with AOT suspensions cannot be explained by the same model developed for PIBS. The different behavior arises from the size difference between AOT and PIBS inverse micelles, resulting in differences in the generation rate and in the interaction with the surface. We propose an equivalent electrical circuit, which explains the measured initial current and the decay rate of the current, for a wide range of surfactant concentrations, device thicknesses, and applied voltages. The components of the equivalent electrical circuit are related to physical properties of the micelles and to the interaction between micelles and the measurement device.

2. MATERIALS AND METHODS

The devices used for the transient current measurements presented in this work consist of two glass plates, coated with an indium tin oxide electrode (ITO) with overlapping surface area $S = 1 \text{ cm}^2$. Glass spacer balls mixed with ultraviolet curing glue (Norland) hold these two electrodes separated at a distance d . Devices were made with thicknesses $d = 5, 19, 32$, and $56 \mu\text{m}$. In each case, the thickness was determined from the interference fringes in the transmission spectrum, measured with a spectrophotometer (Perkin-Elmer, Lambda 35). The space between the electrodes is filled with a mixture of high-purity (99.9%) *n*-dodecane (dielectric constant $\epsilon_r = 2$) (VWR) and the surfactant AOT (Sigma-Aldrich) with mass fraction of $\phi_m = 0.01, 0.03$, and 0.1 of AOT/dodecane, or respectively, $17, 51$, and 174 mM . No measures were taken to eliminate traces of water in the mixtures; comparison of the conductivity in our results with other studies in which the water content was minimized shows that this does not have a significant influence on the results.¹⁶

AOT molecules have two nonpolar tails and an anionic polar head-group. In dodecane, they form inverse micelles above the critical micelle concentration (cmc), which is 1 mM .¹⁶ In all the devices used for the measurements in this work, we are well above the cmc and the low concentration of charged inverse micelles, which leads to low generation rate and conductivity of the solution.²⁸ AOT inverse micelles in dodecane are spherical with a hydrodynamic radius $r_M = 1.6 \text{ nm}$, and the average number of surfactant molecules in each micelle is approximately 22 .^{16,18} A small fraction $\chi = 1.5 \times 10^{-5}$ of the micelles are (positively or negatively) charged.¹⁵ Because of the strong electrostatic interaction in nonpolar liquids, the majority of the inverse micelles are univalently charged. The mobility μ of the charged inverse micelles can be estimated from their hydrodynamic radius: $\mu = q_e / 6\pi\eta r_M$, where q_e is the elementary charge and η is the viscosity of the medium (for dodecane, $\eta = 1.4 \times 10^{-3} \text{ kg}\cdot\text{m}^{-1}\cdot\text{s}^{-1}$). Using the hydrodynamic radius of the inverse micelles of 1.6 nm reported in the literature,^{15,16} the mobility of charged AOT inverse micelles can be estimated to be $\mu = 3.8 \times 10^{-9} \text{ m}^2\cdot\text{V}^{-1}\cdot\text{s}^{-1}$. The measured conductivity of the AOT/dodecane

solutions of about 530 nS/m per mass fraction of AOT added to dodecane (see next section) is similar to values reported elsewhere.^{15,16}

Before each series of transient current measurements, the electrodes are short-circuited for a sufficient amount of time ($10\,000 \text{ s}$) to ensure equilibrium conditions. Then, a voltage difference V_A is applied across the electrodes and the external transient “polarizing” current ($0 \rightarrow V_A$) is measured using a Keithley 428 current amplifier. We performed measurements for the voltage steps $V_A = 0.01, 0.02, 0.05, 0.1, 0.2, 0.5, 1, 2$, and 5 V . After 1000 s , the voltage is reversed ($V_A \rightarrow -V_A$), and the transient “reversal” current is measured. Finally, the cell is short-circuited again, and the transient “relaxation” current ($-V_A \rightarrow 0$) is measured. The level of the currents is always well above the detection limit of the electrometer, which is lower than 1 pA .

3. RESULTS

A typical series of transient polarizing ($0 \rightarrow V_A$), reversal ($V_A \rightarrow -V_A$), and relaxation current ($-V_A \rightarrow 0$) measurements is shown in Figure 1 (a, b, c), for a device with thickness $32 \mu\text{m}$, filled with mass fraction $\phi_m = 0.03$ AOT in dodecane, and for $0.01, 0.02, 0.05, 0.1$, and 0.2 V . On this semilogarithmic scale, it is clear that the transient currents decrease exponentially, with the same time constant, for all applied voltages. The same behavior was observed for devices with different thicknesses ($d = 5, 19, 32$, and $56 \mu\text{m}$) and different mass fractions of AOT ($\phi_m = 0.01, 0.03$, and 0.1). The initial current of these measurements is summarized in Figure 1d as a function of the applied voltage V_A . It shows that the initial polarizing and relaxation currents are the same over a wide range of applied voltages. The initial reversal current is about twice as high as the initial polarizing or relaxation currents for all applied voltages.

In earlier work, we showed that, for mixtures of dodecane with the surfactant PIBS, the transient currents at short times can be explained with a model using drift and diffusion of charged inverse micelles. In some situations, this model predicts an exponential decrease of the current. In many cases, however, especially for the higher voltages, the model with drift and diffusion predicts a linear or power law decrease. Our measurements for the AOT/dodecane mixture show that it behaves different from the PIBS/dodecane mixture.

The exponential decrease of the transient current is characterized by the initial current I_0 and the time constant τ . These parameters are estimated by fitting the measured currents to an exponential, using a logarithmic least-squares method. Figure 2 shows how the initial current of the polarizing current ($0 \rightarrow V_A$) varies with the voltage, the thickness of the device, and the AOT/dodecane mass fraction. The initial current is found to be proportional to the voltage and the mass fraction of AOT/dodecane, and inversely proportional to the thickness

$$I_0 \approx \phi_m V_A / d \quad (2)$$

If we assume that, after short-circuiting the device, the concentrations of positively and negatively charged inverse micelles are homogeneously distributed and equal to \bar{n} , and that the electric field is homogeneous and equal to V_A/d , the initial current can be expressed as^{23,24}

$$I_0 = 2q_e \bar{n} \mu S V_A / d \quad (3)$$

From this, the observed relation in eq 2 is expected knowing that the conductivity $\sigma = 2q_e \bar{n} \mu$ is proportional to the mass fraction ϕ_m of AOT in dodecane.^{15–17} The fitted linear trend line in Figure 2 shows that the conductivity is $\sigma = 530 \text{ nS m}^{-1} \times \phi_m$

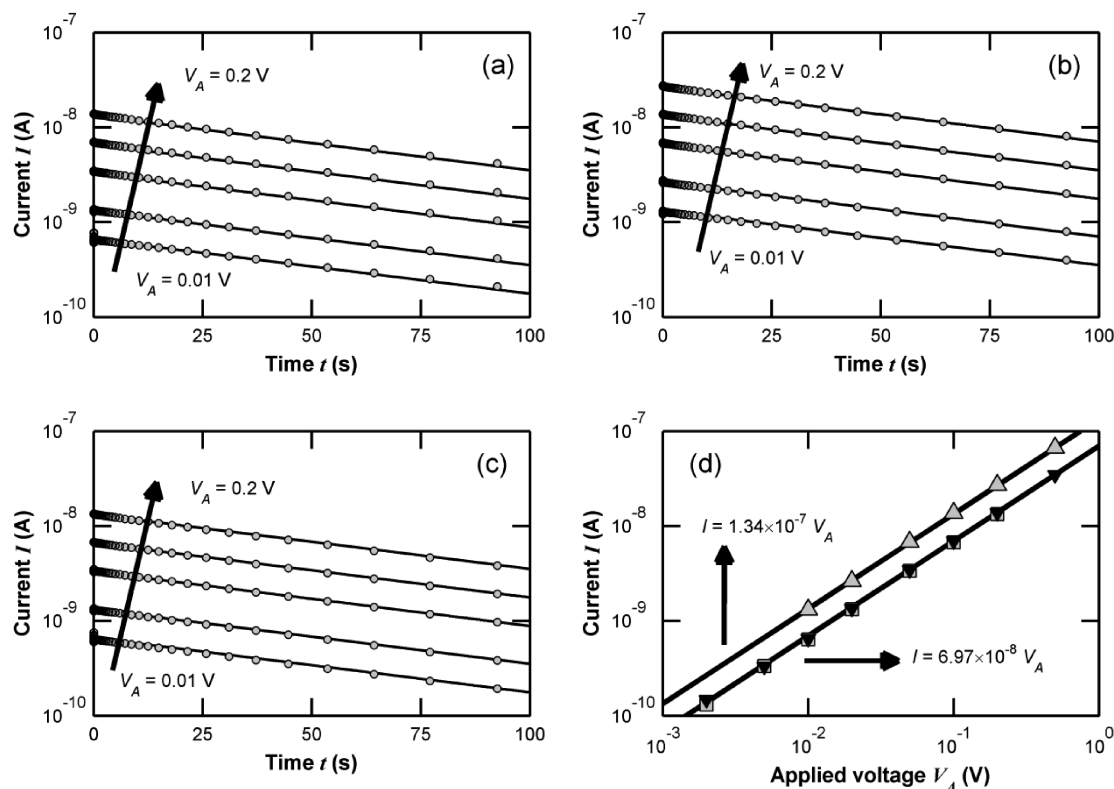


Figure 1. Transient current measurements (dots) for a cell with $\phi_m = 0.03$ surfactant AOT in dodecane, with $d = 32 \mu\text{m}$ and $S = 1 \text{ cm}^2$, for different applied voltages: (a) “polarizing” currents ($0 \rightarrow V_A$), (b) “reversal” currents ($V_A \rightarrow -V_A$), and (c) “relaxation” currents ($-V_A \rightarrow 0$), with $V_A = 0.01, 0.02, 0.05, 0.1$, and 0.2 V . The solid lines show the exponential fit based on a logarithmic least-squared method; (d) Initial current for polarizing (▼), reversal (▲), and relaxation (■) current as a function of applied voltage.

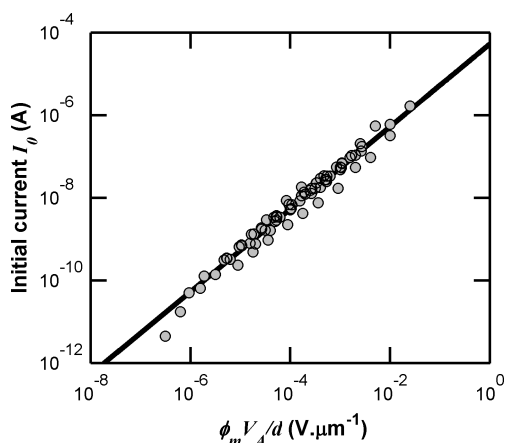


Figure 2. Measured initial current (dots) for $0 \rightarrow V_A$, for different mass fractions of AOT/dodecane ($\phi_m = 0.01$ and 0.03) and different thicknesses ($d = 5, 19, 32$ at $56 \mu\text{m}$) at voltages ($V_A = 0.01, 0.02, 0.05, 0.1, 0.2, 0.5, 1, 2$, and 5 V), plotted vs $\phi_m V_A / d$.

for the mass fractions of 0.01 and 0.03 . Above around $\phi_m = 0.1$, the conductivity increases more than proportionally with the mass fraction, which is also reported elsewhere.¹⁶

Figure 3 shows the time constants τ for the $\phi_m = 0.1$ AOT solution in devices with $d = 5$ and $19 \mu\text{m}$, and for the $\phi_m = 0.03$ AOT solution in devices with $d = 19$ and $56 \mu\text{m}$ as a function of the applied voltage. It is clear that the time constant does not depend on the applied voltage. The same conclusion was found

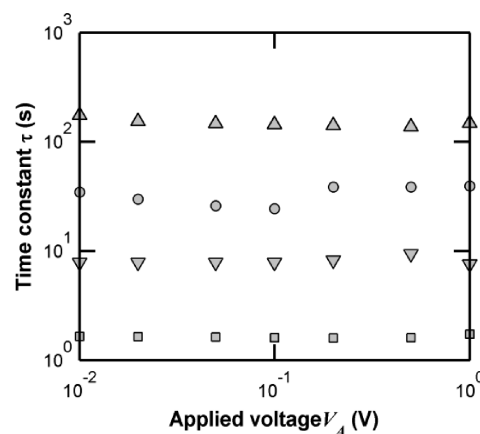


Figure 3. Exponential decay time constant extracted from the current measurements $0 \rightarrow V_A$ as a function of the applied voltage for $\phi_m = 0.1$ AOT/dodecane with $d = 5 \mu\text{m}$ (■) and $d = 19 \mu\text{m}$ (▼), and for $\phi_m = 0.03$ AOT/dodecane with $d = 19 \mu\text{m}$ (●) and $d = 56 \mu\text{m}$ (▲).

for devices with different thicknesses and mass fractions of AOT/dodecane and for polarizing, reversal, and relaxation currents. From measurements on devices with other thicknesses and mass fractions shown in Figure 4, we conclude that the time constant is proportional to the thickness of the device and inversely proportional to the mass fraction of AOT surfactant

$$\tau \approx d / \phi_m \quad (4)$$

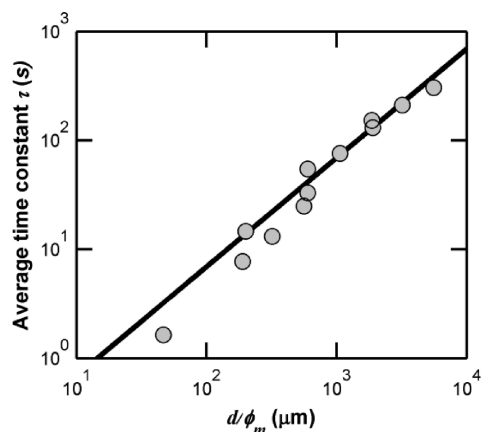


Figure 4. Exponential decay time constant averaged over all applied voltages ($0 \rightarrow V_A$), for samples with different thicknesses ($d = 5, 19, 32$, and $56 \mu\text{m}$) and with different mass fractions of AOT ($\phi_m = 0.01, 0.03$, and 0.1), as a function of d/ϕ_m .

This trend as well as the physical meaning of the time constant is explained in the Discussion section. The linear trend line fitted to the data in Figure 4 can be described by $\tau = (6.90 \times 10^{-4} \text{ s m}^{-1}) \times d/\phi_m$. For sufficiently long times ($t \gg \tau$) and for high enough voltages ($V_A > kT/q_e$, with Boltzmann constant k and temperature T), the exponential decay is halted and the current reaches a quasi-steady-state value (not shown in the measurements), but this behavior is beyond the scope of this paper.

4. DISCUSSION

4.1. Equivalent Circuit Model. The exponential decay of the transient currents and the dependencies in Figures (1–2'3'4) are consistent with an equivalent RC circuit model. The fact that the polarizing and relaxation currents have the same magnitude and the reversal current is twice as high (Figure 1d) shows that the charge transferred during one pulse is stored and can be reversed during the next pulse. This indicates that there is no significant electrochemistry at the electrode surface. The model we propose is shown in Figure 5. The resistance of the ITO electrodes and of the bulk solution is represented by R_{ITO} and R_{bulk} , respectively. The capacitance of the bulk is $C_{\text{bulk}} = \epsilon_0 \epsilon_r S/d_{\text{bulk}}$ in which ϵ_r is the relative dielectric constant of the AOT/dodecane suspension, assumed to be 2 as for pure dodecane. The thickness of the bulk, d_{bulk} , is in good approximation equal to the thickness of the device d . The exponential decay of the current can be characterized by an interface capacitance C_i at the electrode/liquid interface with the thickness of d_i , which is proportional to the electrode area. The combination of two interface capacitances in series with the bulk components is represented by $C_i/2$. The two bulk components R_{bulk} and C_{bulk} (that are parallel with each other) are therefore in series with $C_i/2$ and R_{ITO} .

Because the capacitance of the bulk is much smaller than C_i and the resistance of ITO is much smaller than that of the bulk, the values R_{ITO} and C_{bulk} can be set to zero. In this case, the current as a result of a voltage step V_A is that of a simple RC circuit

$$I_{0 \rightarrow V}(t) = \frac{V_A}{R_{\text{bulk}}} e^{-t/(R_{\text{bulk}} C_i/2)} \quad (5)$$

with $\tau = R_{\text{bulk}} C_i/2$ the time constant of the decay. If we

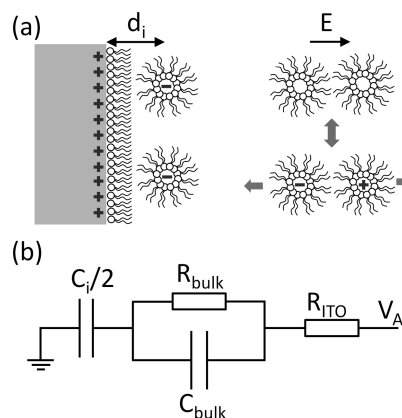


Figure 5. (a) Schematic model near the positively charged interface; (b) equivalent circuit: R_{bulk} and C_{bulk} are the resistance and the capacitance of the bulk solution, R_{ITO} corresponds to the resistance of the ITO electrodes, and $C_i/2$ is formed by two interface capacitances in series.

combining eq 5 at $t = 0$ with eq 3, it follows that the resistance of the solution R_{bulk} depends on the conductivity $2\pi q_e \mu$ of the solution, the thickness of the bulk d , and the area S

$$R_{\text{bulk}} = V_A/I_0 = d/(2\pi q_e \mu S) \quad (6)$$

The value of R_{bulk} is obtained from the measurements by dividing the initial current by the applied voltage. The average value for all measurements can be represented by $R_{\text{bulk}} = (1.88 \text{ M}\Omega \text{ m}) \times d/(S\phi_m)$.

By dividing the decay time by the resistance of the bulk, the value of C_i can be estimated. By combining eqs 4 and 6, we find that $C_i = 2\tau/R_{\text{bulk}}$ should be independent of the AOT/dodecane mass fraction, device thickness, or applied voltage. In Figure 6, it can indeed be observed that C_i obtained from the polarizing transients ($0 \rightarrow V_A$) is more or less independent of the mass fraction of AOT, the thickness of the device, and the voltage. The interface capacitance per unit area has the average value of $C_i = 9.56 \times 10^{-2} \text{ F/m}^2$. A similar value is obtained for the reversal and relaxation currents.

The RC circuit model also allows us to estimate the current for reversing the voltage. In this case, there is an initial charge $C_i V_A$ on the capacitance C_i , and the current supplied to the circuit is

$$I_{V \rightarrow -V}(t) = \frac{-2V_A}{R_{\text{bulk}}} e^{-t/(R_{\text{bulk}} C_i/2)} \quad (7)$$

which is an exponential with a two times higher initial current and the same time constant as for the polarizing current which is compatible with the measurements (such as in Figure 1). In the relaxation step, by applying 0 V, both interface capacitors C_i are discharged through the resistor R_{bulk} , and from the model, the current should be

$$I_{-V \rightarrow 0}(t) = I_0 e^{-t/\tau} = \frac{V_A}{R_{\text{bulk}}} e^{-t/(R_{\text{bulk}} C_i/2)} \quad (8)$$

which is the same as eq 5. It can indeed be observed that the polarizing and relaxation currents in Figure 1a,c behave identically, as confirmed by the data in Figure 1d. The same experiments have been repeated using two bare gold (Au) electrodes instead of ITO. The results for the Au electrodes are similar to those obtained for the ITO electrodes, but with a lower capacitance for C_i ($2.98 \times 10^{-2} \text{ F/m}^2$).

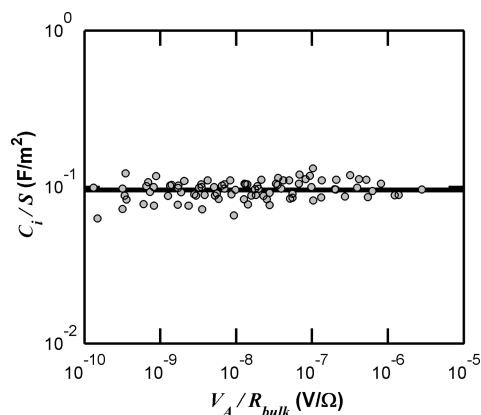


Figure 6. Capacitance per unit area C_i/S as function of V_A/R_{bulk} for all applied voltages (only from the polarizing transients: $0 \rightarrow V_A$), for samples with different thicknesses ($d = 5, 19, 32$, and $56 \mu\text{m}$) and with different mass fractions of AOT/dodecane ($\phi_m = 0.01, 0.03$, and 0.1).

4.2. Physical Interpretation. The fact that the bulk of the liquid in our devices can be approximated well by a simple resistance R_{bulk} indicates that the conductivity of the AOT/dodecane mixtures remains constant over time when a voltage is applied. This is contrary to the situation for PIBS/dodecane, in which the separation (and even depletion at voltages much higher than the thermal voltage) of charged inverse micelles results in a decrease of the conductivity when a voltage is applied.^{23,24,29} We conclude that the generation rate of charged inverse micelles is much higher in AOT/dodecane than in PIBS/dodecane, resulting in an almost immediate replenishment of charge carriers in the bulk. In fact, the dynamics of the disproportionation/comproportionation reaction^{15–17,24} should be sufficiently fast to maintain the equilibrium concentration of charged inverse micelles at high electric fields.

For dodecane with high concentrations of PIBS and relatively low applied voltages, the transient current decreases considerably within the so-called diffuse double layer time $t_{\text{DL}} = d\lambda_{\text{DL}}/2D$ (with λ_{DL} the Debye length and D the diffusion constant of the charged inverse micelles),²³ because the formation of a double layer with thickness λ_{DL} screens the electric field in the bulk. However, in the experiments with dodecane and AOT, even at low voltages, there is no sign of screening of the electric field corresponding to the Debye double layer capacitance. For example, in the case of 0.03 mass fraction of AOT in dodecane corresponding to a concentration of charged inverse micelles of $1.8 \times 10^{19} \text{ m}^{-3}$ in a device with $d = 56 \mu\text{m}$ (see Figure 3), the Debye length is about 400 nm and the time constant t_{DL} of 0.15 s is much smaller than the experimentally observed decay time $\tau = 170$ s. This indicates that the charged inverse micelles do not form an extended (Debye) diffuse double layer, but move much closer to the electrode and remain there as in a Helmholtz layer which can be modeled as a capacitor.³⁰ From the value of capacitance per unit area, the dielectric constant per unit length can be extracted. Assuming a relative dielectric constant on the order of 10 leads to a distance between the charges and the electrode of 1.0 nm. It is important to mention that surface morphology can affect the device characteristics and consequently the value of the interface capacitance, because high roughness increases the effective area. This might explain why for flat bare gold electrodes the interface capacitance ($2.98 \times 10^{-2} \text{ F/m}^2$) is smaller than for ITO ($9.56 \times 10^{-2} \text{ F/m}^2$) which is known to be rather rough.³¹ In both

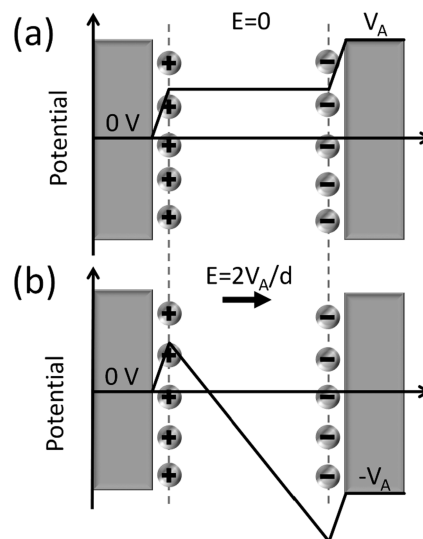


Figure 7. Schematic illustration of the variation of the potential in the presence of a layer of AOT charged inverse micelles at the end of the transient of the polarizing step, $0 \rightarrow V_A$ (a), and immediately after switching the voltage in the reversal step $V_A \rightarrow -V_A$ (b).

devices, it is observed that the charged inverse micelles remain near the electrode, which can be explained by the attractive force of its mirror charge. For small inverse micelles, we indeed expect the electrostatic binding energy to be larger than their thermal energy. Another possible explanation would be the formation of a layer of surfactant (similar to a bilayer) containing charged species.

At the end of the transient current, large amounts of charged inverse micelles are present near the electrodes. When the voltage is reversed, we observe that the current is simply two times larger than for the first transient (Figure 1d). Superposition of the field induced by the inverse micelles (which lead to the complete screening of the field at the end of the polarizing transient in Figure 7a) and the field caused by the reversed applied voltage $-V_A$ leads to a field in the bulk which is twice as high as in the beginning of the polarizing transient (Figure 7b). As a result, the charged inverse micelles in the bulk move at the double speed, leading to a double current, as evidenced in (b) and (d) of Figure 1. For the reverse transient, the field in the bulk is twice as high, and two times as much charge has to be transported from the bulk to the interfaces with the electrodes to again reach complete screening. As a result, the time constant for screening is the same.

In the model described above, the focus is on the final result: a current density in the bulk and the charges ending up near the interfaces. In fact, the detailed picture is more complicated. In the absence of a field, positive and negative inverse micelles continuously collide with the electrodes, and many of them stick to the interfaces. At the same time, oppositely charged inverse micelles that stick on the electrode attract each other and may annihilate into two uncharged inverse micelles, which do not necessarily stick to the surface anymore. So, in the steady state, there is an equilibrium surface concentration of charged inverse micelles at the electrodes. When a voltage is applied, this equilibrium is broken, and there is a net flux of charged micelles toward the interfaces. In this case, the net flux of one polarity of inverse micelles (for example, positive inverse micelles near the

negative electrode) will mainly build up the Helmholtz layer on the electrode. This is because we assume that only uncharged inverse micelles can leave the interface, while charged micelles (if they do not annihilate with an inverse micelle of opposite polarity) stay at the surface.

5. CONCLUSION

The transient current caused by charged inverse AOT micelles in dodecane behaves differently from the transients observed for inverse PIBS micelles in dodecane, and cannot be modeled by drift diffusion and generation alone. Because of the small size of AOT micelles, the generation rate is high and leads to a charge density in the bulk of the solution which is independent of field, position, and time (it only depends on the mass fraction of AOT/dodecane). Due to their small size, the AOT charged inverse micelles remain close to the electrodes, and as a result of the strong interaction with their image charges, they remain there even after reversing the voltage. We have presented a simple analytical model with only a few parameters that describes the external current in response to an applied voltage step. Current measurements are reported for different device thicknesses, different voltages, and different mass fractions of AOT/dodecane. All measurements can be reproduced with the analytical model.

AUTHOR INFORMATION

Corresponding Author

*E-mail: mkarvar@elis.ugent.be.

ACKNOWLEDGMENT

This work has partially been sponsored by the IAP-VI-10 project photon@be funded by BELSPO, the Belgian Science Policy program and the Center for Nano- and Biophotonics at Ghent University. F.S. is a Postdoctoral fellow of the Research Foundation – Flanders (FWO Vlaanderen).

REFERENCES

- (1) Blagovidov, I. F.; Lapin, V. P.; Trofimova, G. L.; Shor, G. I. *Chem. Technol. Fuels Oils* **1971**, 7 (6), 439–443.
- (2) Morrison, I. D. *Colloids Surf., A* **1993**, 71 (1), 1–37.
- (3) Pearlstine, K. A. *J. Imaging Sci.* **1991**, 35 (5), 326–329.
- (4) Comiskey, B.; Albert, J. D.; Yoshizawa, H.; Jacobson, J. *Nature* **1998**, 394 (6690), 253–255.
- (5) Chen, Y.; Au, J.; Kazlas, P.; Ritenour, A.; Gates, H.; McCreary, M. *Nature* **2003**, 423 (6936), 136–136.
- (6) Bert, T.; De Smet, H.; Beunis, F.; Neyts, K. *Displays* **2006**, 27 (2), 50–55.
- (7) Mürau, P.; Singer, B. *J. Appl. Phys.* **1978**, 49 (9), 4820–4829.
- (8) Kazlas, P. T.; McCreary, M. D. *MRS Bull.* **2002**, 27 (11), 894–897.
- (9) Kim, C. A.; Joung, M. J.; Ahn, S. D.; Kim, G. H.; Kang, S.-Y.; You, I.-K.; Oh, J.; Myoung, H. J.; Baek, K. H.; Suh, K. S. *Synth. Met.* **2005**, 151 (3), 181–185.
- (10) Novotny, V.; Hopper, M. A. *J. Electrochem. Soc.* **1979**, 126 (12), 2211–2216.
- (11) Meng, X.; Tang, F.; Peng, B.; Ren, J. *Nanoscale Res. Lett.* **2010**, 5 (1), 174–179.
- (12) Kitabara, A.; Amano, M.; Kawasaki, S.; Kon-no, K. *Colloid Polym. Sci.* **1977**, 255 (11), 1118–1121.
- (13) Poovarodom, S.; Berg, J. C. *J. Colloid Interface Sci.* **2010**, 346 (2), 370–377.
- (14) Sainis, S. K.; Germain, V.; Mejean, C. O.; Dufresne, E. R. *Langmuir* **2008**, 24 (4), 1160–1164.
- (15) Roberts, G. S.; Sanchez, R.; Kemp, R.; Wood, T. A.; Bartlett, P. *Langmuir* **2008**, 24 (13), 6530–6541.
- (16) Hsu, M. F.; Dufresne, E. R.; Weitz, D. A. *Langmuir* **2005**, 21 (11), 4881–4887.
- (17) Sainis, S. K.; Merrill, J. W.; Dufresne, E. R. *Langmuir* **2008**, 24 (23), 13334–13337.
- (18) Kotlarchyk, M.; Huang, J. S.; Chen, S.-H. *J. Phys. Chem.* **1985**, 89 (20), 4382–4386.
- (19) Guo, Q.; Singh, V.; Behrens, S. H. *Langmuir* **2010**, 26 (5), 3203–3207.
- (20) Dukhin, A. S.; Goetz, P. J. *J. Electroanal. Chem.* **2006**, 588 (1), 44–50.
- (21) Strubbe, F.; Beunis, F.; Marescaux, M.; Verboven, B.; Neyts, K. *Appl. Phys. Lett.* **2008**, 93 (25), 254106.
- (22) Kim, J.; Garoff, S.; Anderson, J. L.; Schlangen, L. J. M. *Langmuir* **2005**, 21 (24), 10941–10947.
- (23) Beunis, F.; Strubbe, F.; Marescaux, M.; Beeckman, J.; Neyts, K.; Verschueren, A. R. M. *Phys. Rev. E* **2008**, 78 (1), 011502.
- (24) Strubbe, F.; Verschueren, A. R. M.; Schlangen, L. J. M.; Beunis, F.; Neyts, K. *J. Colloid Interface Sci.* **2006**, 300 (1), 396–403.
- (25) Verschueren, A. R. M.; Notten, P. H. L.; Schlangen, L. J. M.; Strubbe, F.; Beunis, F.; Neyts, K. *J. Phys. Chem. B* **2008**, 112 (41), 13038–13050.
- (26) Neyts, K.; Beunis, F.; Strubbe, F.; Marescaux, M.; Verboven, B.; Karvar, M.; Verschueren, A. R. M. *J. Phys.: Condens. Matter* **2010**, 22 (49), 494108.
- (27) Beunis, F.; Strubbe, F.; Marescaux, M.; Neyts, K.; Verschueren, A. R. M. *Appl. Phys. Lett.* **2010**, 97 (18), 181912.
- (28) Novotny, V.; Hopper, M. A. *J. Electrochem. Soc.* **1979**, 126 (6), 925–929.
- (29) Beunis, F.; Strubbe, F.; Neyts, K.; Verschueren, A. R. M. *Appl. Phys. Lett.* **2007**, 90 (18), 182103.
- (30) Delgado, A. V.; González-Caballero, F.; Hunter, R. J.; Koopal, L. K.; Lyklema, J. *Pure Appl. Chem.* **2005**, 77 (10), 1753–1805.
- (31) Jonda, C.; Mayer, A. B. R.; Stoltz, U.; Elschner, A.; Karbach, A. *J. Mater. Sci.* **2000**, 35 (22), 5645–5651.